Available online at www.sciencedirect.com
SCIENCE DIRECT®
Carbohydrate Research 339 (2004) 1007–1014
Carbohydrate RESEARCH

Molecular modeling insights into the catalytic mechanism of the retaining galactosyltransferase LgtC

Igor Tvaroška*

Institute of Chemistry, Slovak Academy of Sciences, Bratislava 845-38, Slovak Republic

Received 25 September 2003; accepted 17 November 2003

Abstract—The bacterial enzyme lipopolysaccharyl α-galactosyltransferase C (EC 2.4.1.x, LgtC) is involved in the synthesis of lipooligosaccharides displayed on the cell surfaces of *Neisseria meningitidis*. LgtC catalyzes the transfer of a galactosyl residue from UDP-Gal to the terminal galactose residue of glycoconjugates with an overall retention of stereochemistry at the anomeric center. Several hypothetical catalytic mechanisms of the LgtC enzyme were examined herein using DFT quantum chemical methods up to the B3LYP/6-311++G**//B3LYP/6-31G* level. The computational model used to follow the reaction is based on the crystallographic structure of LgtC in complex with both the nucleotide–galactose donor and the oligosaccharide-acceptor analogues. The 136 atoms included in this model represent fragments of residues critical for the substrate binding and catalysis. From our calculations, the preferred pathway is predicted to be a one step mechanism with the nucleophilic attack of the acceptor oxygen onto the anomeric carbon and the proton transfer to a phosphate oxygen occurring simultaneously. This mechanism has an $A_ND_NA_HD_H$ character, with the unique transition state structure in which the attacking galactose group is more closely bound to the anomeric carbon than to the UDP leaving group and where the hydrogen bond between the nucleophile and the leaving group oxygens facilitates the attack of the acceptor O4′ from the same side of the transferred galactose.

Keywords: Retaining glycosyltransferases; LgtC; Catalytic mechanism; Reaction pathways; Transition state; $A_ND_NA_HD_H$ mechanism

1. Introduction

Glycosyltransferases are enzymes that transfer a glycosyl residue from an activated donor to an acceptor. In the past few years, several three-dimensional structures of glycosyltransferases have been reported in the literature.[1–15] The catalytic reaction catalyzed by a glycosyltransferase can proceed with either inversion or retention of configuration at the anomeric carbon of the donor. In the case of inverting glycosyltransferases, the available structural information[16,17] and theoretical calculations[18,19] support a single nucleophilic displacement of the nucleotide by one of the hydroxyl groups of the acceptor. On the other hand, the commonly assumed double-displacement mechanism of retaining glycosyltransferases remains unsupported by all available X-ray structures of retaining glycosyltransferases. Theoretical investigations[20] of various possible reaction pathways describing a double-displacement mechanism indicate that the energetically most favorable pathway requires the presence of only one catalytic acid in the active site with the UDP functioning as a general base in the second step of the reaction (Scheme 1).

Lipopolysaccharyl α-galactosyltransferase C (EC 2.4.1.x, LgtC) from *Neisseria meningitidis* is the enzyme catalyzing the transfer of a galactosyl residue from uridine diphosphogalactose (UDP-Gal) to a galactose of the terminal lactose moiety on the bacterial lipopolysaccharide and is therefore a potential target for a treatment of infections caused by this microorganism.[8,21] This catalytic reaction yields an elongated oligosaccharide product with net retention of the anomeric configuration relative to the donor, which is characteristic of retaining glycosyltransferases. The overall catalytic reaction is illustrated in Scheme 2. On the basis of sequence similarities, LgtC belongs to family 8 of

* Tel.: +421-2-59410322; fax: +421-2-59410222; e-mail: chemitsa@savba.sk

0008-6215/$ - see front matter © 2003 Elsevier Ltd. All rights reserved.
doi:10.1016/j.carres.2003.11.014

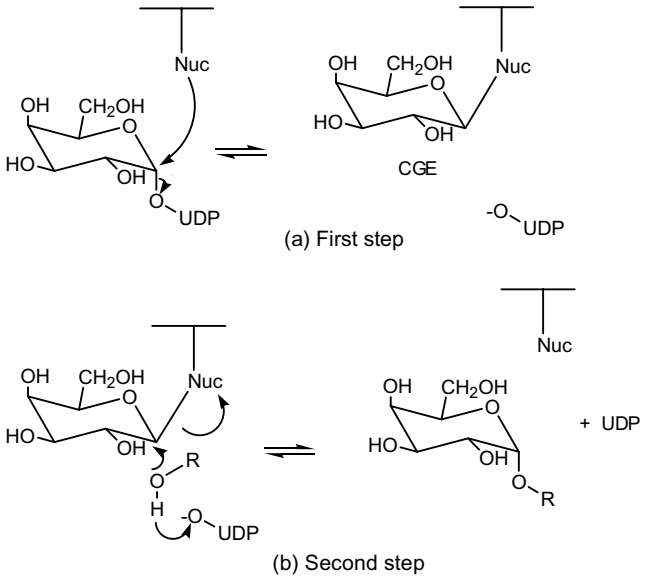

Scheme 1. Schematic representation of the (a) first step and (b) second step of the proposed mechanism[20] for retaining glycosyltransferases via a double-displacement mechanism.

glycosyltransferases[22] and the crystal structure of the complex of LgtC with manganese and UDP 2-deoxy-2-fluorogalactose (a donor substrate analogue) in the presence and absence of the acceptor sugar analogue 4′-deoxylactose were recently solved[8] at 2 Å. Experiments have shown[21] that LgtC follows an ordered bi–bi kinetic mechanism in which UDP-Gal binds first, followed by the acceptor lactose. The enzyme catalyzing the reaction of UDP-Gal with lactose to give UDP and a trisaccharide occurs with apparent second-order rate constants[8,21] ranging from 14 to 34 s^{-1}, which correspond to energy barriers of about 12–14 kcal/mol. It was found[21] that the enzyme does not bind very tightly to the acceptor ($K_m = 60$ mM), while the donor UDP-Gal does bind very strongly ($K_m = 18$ μM). After the reaction, the trisaccharide leaves first the reaction site followed then by UDP. The difficult identification of a catalytic base in the active site of LgtC as well as the absence of any convincing evidence for the existence of a covalent intermediate has led to the suggestion that this enzyme might rather proceed through a single front-side displacement reaction, also known as an S_Ni mechanism and previously invoked for glycogen phosphorylases.[23] The lack of experimental evidences however does not permit yet to clearly conclude on the actual type of mechanism involved.

We report here a theoretical study of the mechanism of the bacterial LgtC. Several hypothetical reactions were examined for this enzyme using nonempirical quantum chemical methods. Studies using similar techniques have already been published on the mechanism of inverting *N*-acetylglucosaminyltransferases[18,19] and on the double-displacement mechanism of retaining glycosyltransferases.[20] Understanding the reaction mechanism of LgtC and the determination of the transition state structure is a prerequisite for the design of a potent and specific inhibitor for this enzyme, which could in turn act as new antibiotics.

2. Model and computational procedures

The starting point for the reaction site model was the crystallographic structure[8] of LgtC in complex with manganese, UDP 2-deoxy-2-fluoro-galactose and 4′-deoxylactose, which was resolved at 2 Å (code number 1GA8 in Protein Data Bank, PDB). Both substrate analogues were transformed into the native substrates, UDP-galactose and lactose, respectively. Our structural model of the reaction site included all relevant parts of the donor and acceptor substrates, the metal cofactor, and key amino acids involved either in the enzymatic reaction or in the binding of the substrates with the geometrical features observed in the crystal structure. A schematic representation of the reaction site model is shown in Scheme 3. The model contained 136 atoms consisting of the complete sugar-donor molecule, UDP-Gal; a galactose derivative representing the oligosaccharide acceptor; the divalent metal cofactor Mn^{2+} modeled by Mg^{2+}, which has the same preferred coordinate number as manganese and both metals behave similarly.[24] Divalent magnesium is fully coordinated by aspartate D103, aspartate D105, and histidine H244, as found in the X-ray structure; a portion of glutamine Q189 presumed to be the catalytic base in one of assumed mechanisms; and the essential fragment of aspartate D8 interacting with the uridine part of the

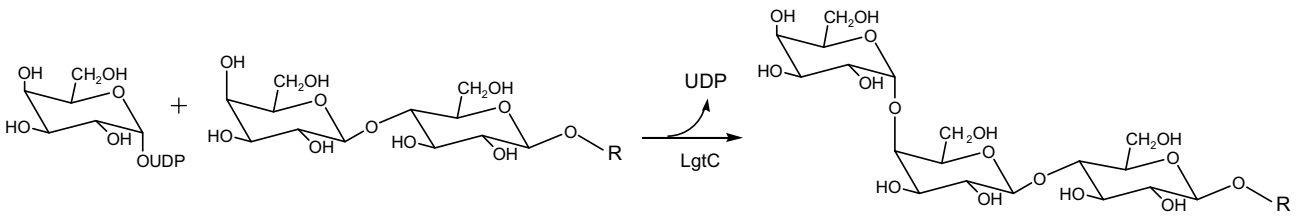

Scheme 2. Schematic representation of the galactosyl transfer from UDP-Gal to the LPS core oligosaccharide of *N. meningitidis* catalyzed by the retaining LgtC.

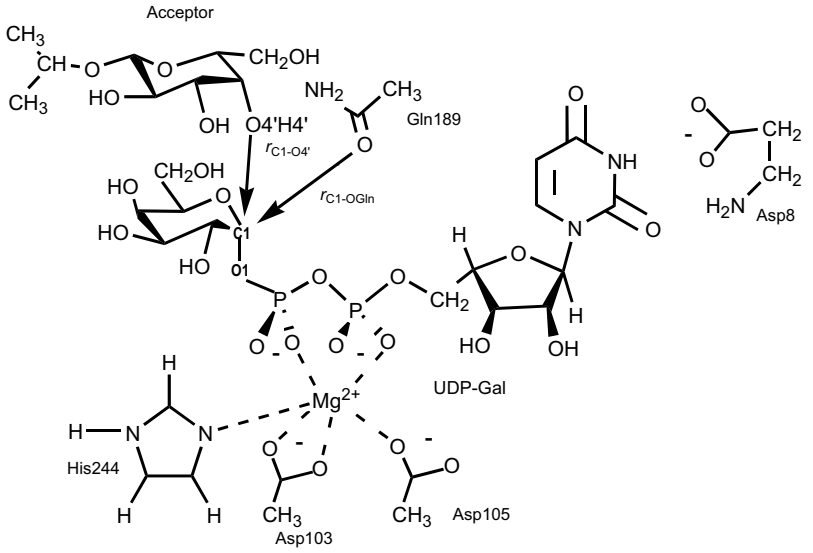

Scheme 3. Schematic representation of the structural model used to investigate the reaction catalyzed by LgtC.

donor. With this reaction-site model we have explored computationally different reaction hypotheses for the galactosyl transfer catalyzed by LgtC. Calculations were carried out using the Jaguar program.[25] Optimization of the geometry was performed using the B3LYP density functional method[26] with the 6-31G* basis set (1259 basis functions). Geometries of all stationary points on the PES were then fully optimized with no constraints on the reaction coordinates. The exceptions were coordinates defining the location of α-carbons of the enzyme amino acids that were constraint to their crystallographic positions. The structure of the transition state was calculated using the three nearest points to the particular barrier on the PES using the QST-guided search of the Jaguar software.[25] Finally, single point energy calculations were performed on selected geometries determined at the B3LYP/6-31G* level using the B3LYP/6-31++G** and B3LYP/6-311++G** basis sets (1803/2101 basic functions), respectively.

3. Results and discussion

The catalytic mechanism of retaining glycosyltransferases via a double-displacement mechanism[27] proceeds in two steps and requires the presence of two catalytic residues in the vicinity of the reaction site. The first step is the formation of a covalent glycosyl–enzyme complex (CEG) between the enzyme catalytic base and the sugar of the donor with inverted configuration at the anomeric carbon atom of the donor. The catalytic acid is also involved in this step to facilitate the departure of the leaving group UDP by protonating the glycosidic oxygen. In the second step of this mechanism, the catalytic acid becomes a proton acceptor of the acceptor hydroxyl group, which is performing the second inverting nucleophilic attack at the anomeric carbon resulting in a product with retaining configuration. To date, all experimental structures of glycosyltransferases, except LgtC, showed the presence of only one catalytic acid in the active site. Theoretical investigations, in agreement with these structural data, indicate that the most favorable model of the mechanism requires the presence of only one catalytic acid involved in the formation of the CEG in the active site and UDP functioning as a general base in the second step of the reaction (Scheme 1). In the X-ray structure of the LgtC complexes, however, only Gln189 is within a suitable distance to act as the catalytic acid. Several electronegative groups in the vicinity of the UDP-Gal were considered as possible catalytic nucleophiles[8,21] but the analysis of the results was inconclusive and the catalytic mechanism of LgtC therefore remains a puzzle. To shed some light on this specific case of the catalytic mechanism of retaining glycosyltransferases, we have examined various reaction hypothesis of the galactosyl transfer catalyzed by LgtC and results will be discussed consecutively.

3.1. Reaction pathways calculations

As in our previous studies,[18–20] we have calculated potential energy surfaces for the enzyme mechanism as a function of distances, which we considered could well describe the particular reaction. Two distances were used as reaction coordinates (Scheme 3): the $r_{C1–O4'}$ distance between the anomeric carbon and the oxygen O-4′ of the acceptor hydroxyl group and the $r_{C1–OGln}$ distance between the anomeric carbon and the oxygen O-Gln of the Gln189 amino acid. These geometrical variables reflect the nucleophilic attack of a potential

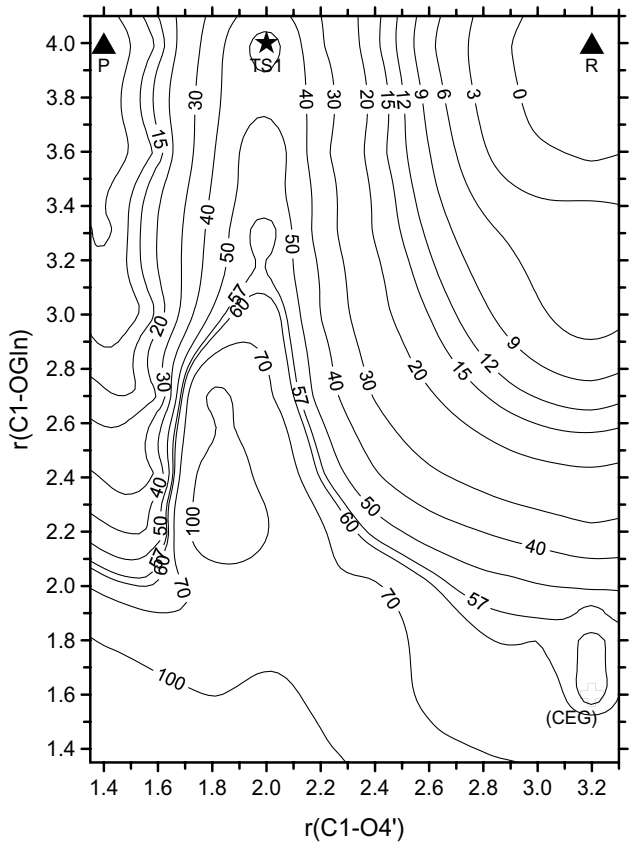

Figure 1. PES calculated at the B3LYP/6-31G* level as a function of the $r_{C1-O4'}$ and $r_{C1-OGln}$ distances.

nucleophile on the anomeric carbon and permit the description of the bond-breaking and bond-forming processes of the galactose transfer reaction. The B3LYP/6-31G* potential energy surface obtained from the calculations with the $r_{C1-O4'}$ and $r_{C1-OGln}$ distances as reaction coordinates is shown in Figure 1. The calculation of the surface represented by a contour map required 195 restricted optimizations. Each calculated point on the PES corresponds to the optimized structure and the arrangement of the model for the given pair of values of $r_{C1-O4'}$ and $r_{C1-OGln}$ distances, respectively. During the optimization, all geometrical parameters were optimized with the exception of those defining the location of the α-carbon of the enzyme amino acids. As a result, each point on the PES is represented by fixed values of the reaction coordinates, and all points have all their geometrical variables relaxed to their most stable values. The location of the local minima and transition barriers on the PES is only approximate, and for that reason a further optimization of stationary points with no constraints on the $r_{C1-O4'}$ and $r_{C1-OGln}$ distances is required. However, to avoid any confusion, we will use throughout the paper the same acronyms for these points.

The PES shows high energy region in the left-bottom corner, which represents unstable pentacoordinated anomeric carbon. There seems to be a pathway from reactants to products, which would proceed via two steps. The first step, describes the reaction coordinate parallel to the vertical axis that characterizes the nucleophilic attack of the Gln189 oxygen on the anomeric C-1 of UDP-Gal and should represent the formation of the covalent galactosyl–Gln189(LgtC) intermediate (covalent enzyme–glycosyl intermediate; CEG). This pathway from the top-right corner to the bottom-right corner of the PES can be regarded as the first step of the double-displacement reaction mechanism. In accordance with this mechanism, the second step involves the breakdown of CEG and the formation of the α-(1 → 4) linkage between the acceptor and galactose. The pathway corresponding to this step would follow the diagonal from the bottom-right corner to products at the top-left corner of the PES. To shed more light on the mechanism we have performed more detailed calculations of the stationary points along the reaction pathway. It turned out that the local minimum at the bottom-right corner of the PES (CEG) does not correspond to the real minimum. A refinement of the local minimum without constraints on the $r_{C1-O4'}$ and $r_{C1-OGln}$ coordinates led to the covalent galactosyl–LgtC intermediate structure with a relative energy about 33 kcal/mol higher compared to the reactants and has an estimated barrier of about 55 kcal/mol. However, the analysis of the geometrical parameters revealed that the C-1–O-4′ distance was quite considerably elongated during the optimization going from the X-ray structure based value[2] of 3.2 to 5.2 Å in CEG. The location of the CEG is outside of borders of the PES presented in Figure 1. The C-1–OGln bond in CEG has the value of 1.47. Moreover, the increase of the C-1–O-4′ distance in CEG is achieved by the rotation of the acceptor residue from its crystallographic orientation, which seems to be a very important structural feature for the outcome of the catalytic reaction. In the crystal structure, this highly ordered orientation of the galactosyl residue in the active site is stabilized by the hydrogen bonds between O-3, O-4, and O-6 and side chains of the enzyme.[8] Indeed, any attempt to follow the nucleophilic attack of O-4′, as a function of the $r_{C1-O4'}$, from the orientation in CEG led to a product either with an open galactose ring or with a β-glycosidic linkage. Therefore we did not attempt to determine the transition state structure for this kind of mechanism. These results suggest that Gln189 does not play the role of an enzymatic nucleophile what implies that this reaction model of the double-displacement reaction mechanism is very unlikely to occur. This might also explain why all attempts to trap the covalent galactosyl–LgtC intermediate were unsuccessful.[21]

There is a direct pathway (R → TS → P) that proceeds in one step. Such a pathway is described by the reaction coordinate plotted along the horizontal axis of the

Table 1. Comparison of the ab initio relative energies (kcal/mol) calculated by various methods for the stationary point of the one step mechanism

Geometry//energy	6-31G*//6-31G*	6-31++G**//6-31G*	6-311++G**//6-31G*
R	0.00[a]	0.00[b]	0.00[c]
TS	51.77	32.25	31.34
P	5.71	−11.81	−11.00

[a] $E = -3{,}060{,}335.39$ kcal mol.
[b] $E = -3{,}060{,}535.16$ kcal mol.
[c] $E = -3{,}061{,}191.05$ kcal mol.

contour map and it involves the nucleophilic attack of the acceptor hydroxyl O-4′ onto the anomeric carbon of UDP-Gal. Analysis of the minimum structure revealed that during the nucleophilic attack of the acceptor oxygen O-4′ on C-1, the C-1–O-1 bond between the galactose and UDP is broken and the H-4′ proton is transferred from the attacking acceptor hydroxyl onto the leaving UDP oxygen O-1. The local minimum at the top-left corner therefore represents the reaction product with the galactose residue transferred from UDP-Gal to O-4′ of the acceptor and linked with the α-(1 → 4) linkage. A concerted proton transfer from the attacking hydroxyl group to a phosphate oxygen was also observed in the second step of a double-displacement mechanism of retaining glycosyltransferases examined in our previous paper.[20] The concerted pathway is predicted to be the most favorable with an estimated barrier of about 50 kcal/mol at the B3LYP/6-31G* level.

To further characterize the galactose transfer via the concerted mechanism, we have located the reactants (R), transition state (TS), and products (P) along this reaction pathway using the B3LYP/6-31G* method. The optimized structures of these stationary points were used to calculate their energy using the B3LYP/6-31++G** and B3LYP/6-311++G** basis sets. The relative energies values are listed in Table 1. It can be seen that enlargement of the basis set has a significant effect on the magnitude of the relative energy of the stationary points. The calculated energy barrier decreases from about 52 kcal/mol at the B3LYP/6-31G* level to 32 kcal/mol at the B3LYP/6-31++G** level, and at our best theory B3LYP/6-311++G** to 31 kcal/mol. The effect of basis set on the relative energy of TS is quite large compared to previously observed changes.[18–20] We assume that interactions in TS, a proper evaluation of which requires inclusion of diffuse functions, are responsible for this effect. The relative energy of the products is also influenced by the basis set. While at the B3LYP/6-31G* level the catalytic reaction is predicted to be endothermic, at larger basis set the reaction is exothermic. Amongst the three stationary points observed along the evaluated pathway, the transition state represents the structure with the most separated charges. This character should be reflected in the most pronounced stabilization by surrounding environment effects. To estimate this effect we have treated the electrostatic environment as a dielectric continuum using the procedure implemented in Jaguar,[25] Calculations were carried out for two different environment represented by cyclohexane ($\varepsilon = 2$) and water ($\varepsilon = 78$) using the 6-31G** basis set, which has been applied successfully for the prediction of pK_a values of a large set of different molecules.[25] Treated this way, the reaction barrier was decreased by 7 and 21 kcal/mol, respectively. After the correction for the electrostatic environment effects, the reaction barrier could be estimated around 10–24 kcal/mol. This should be compared to the experimental value of the catalysis of galactose transfer by the bacterial LgtC, which has been kinetically estimated[8,21] to be between of 12 and 14 kcal/mol. However, it is clear that these values are very approximate and to estimate effects of both the protein and solvent more realistically would require inclusion of the whole enzyme and surrounding water in the calculations.

3.2. Transition state analysis

The selected structural information calculated for the different stationary points, reactants (R), transitions state (TS), and products (P) detected in Figure 1 at the B3LYP/6-31G* level is given in Table 2. The structure of

Table 2. The B3LYP/6-31G* calculated selected geometric parameters of the stationary points of the one step mechanism

	Parameter	R	TS	P
Bond lengths	C1–O1	1.457	2.662	4.286
	C1–O4′	3.500	2.341	1.415
	C1–O5	1.400	1.283	1.420
	C1–H1	1.090	1.078	1.088
	H4′–O4′	0.982	1.088	4.981
	H4′–O1	2.332	1.342	0.985
	O1–O4′	4.009	2.410	4.003
Bond angles	O5–C1–O1	10.5	82.8	77.8
	O5–C1–H1	105.7	113.2	102.4
	O5–C1–O4′	143.3	103.8	112.9
Torsion angles	O5–C1–O1–P	−177.6	−165.7	165.7
	O5–C1–O4′–C4′	−39.8	35.0	59.1
	C5–O5–C1–O1	62.1	52.1	17.2
	C5–O5–C1–O4′	−156.1	105.7	77.9
	C5–O5–C1–C2	−58.1	−22.2	−45.0
	C5–O5–C1–H1	177.2	−164.2	−178.5
	C5–O5–C6–O6	−61.4	−65.1	−64.2

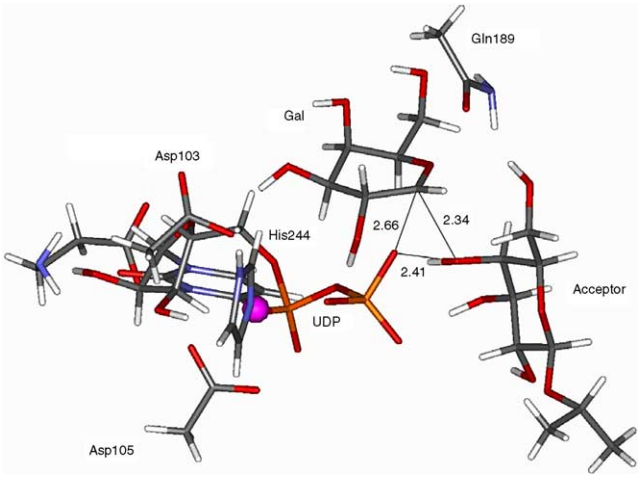

Figure 2. Geometrical representation of the transition state, TS, observed on the PES of Figure 1 and calculated at the B3LYP/6-31G* level.

TS is shown in Figure 2. The transition state structure is characterized by C-1–O-1 and C-1–O-4′ distances of about 2.66 and 2.34 Å, which indicate a loose transition state, but with a significant bond order to both the nucleophile and the leaving group. It can be seen that both the nucleophilic attack by the acceptor oxygen O-4′ and the leaving group departure occur on the same face of the transferred galactose. The nucleophile proton is sandwiched between the oxygens from the phosphate and the nucleophile, which assists the formation of the transition state. The H-4′ proton is located at the O-4′–H-4′ and O-1–H-4′ distances of about 1.09 and 1.38 Å, respectively. The distance between the O-4′ and O-1 oxygens in TS is about 2.4 Å. This resembles the short distances found for low barrier hydrogen bonds, which have an energy of 15–20 kcal/mol and have been postulated to be important in enzyme catalysis.[28] To verify the assistance from the O-1···H···O-4′ hydrogen bond in a stabilization of TS, we have estimated its energy contribution to the overall energy of TS. For this purpose we have rotated H-4′ to a position without any contact with O-1 and the geometry of the O-4′–H-4′ bond was changed to that of a regular O–H bond. The relative energy of such modified TS calculated at the B3LYP/6-31G* level increased to 70.3 kcal/mol, which gave a roughly estimate of 18.5 kcal/mol for the stabilization of TS by this hydrogen bond. The role of this hydrogen bond might be twofold. First, the hydrogen bond energy between the acceptor oxygen O-4′ and the leaving group oxygen O-1 can provide the energy needed to offset the repulsion interactions between the electronegative atoms in TS; second, it facilitates the proton transfer from the attacking to the leaving group. In TS, the ring conformation of the transferred galactose is a distorted ^4E envelope and can be characterized[29,30] by the following linear combination of ideal canonical conformations: $-0.573\,^1C_4 + 0.262\,^{1,4}B + 0.102\,^0S_2$. The anomeric proton is slightly shifted from an ideal orientation in the plane defined by O-5, C-1, and C-2 atoms, as found in the previously determined transition state structures,[18–20] to a quasi-equatorial orientation. This may be attributed to steric constraints of the binding site, particularly the position of both the nucleophile and the leaving groups on the same side.

In addition to the transition state structure, it is interesting to look at how the geometry of the system changes along the reaction pathway. Analysis of the geometrical changes clearly showed that principal movements in the galactose transfer occur around the anomeric carbon atom. The mechanism with the similar motion has been recently described for the *N*-riboyltransferases[31] and retaining glycosidases.[32] In general, the geometry of the remaining atoms changes modestly. The geometry of UDP and the chelation of magnesium remain the same throughout the pathway with the exception of the conformation of the pyrophosphate group changing as the C-1–O-1 distance elongates and the acceptor proton is transferred. Values given in Table 2 show the formation of the C-1–O-4′ bond, going from as far apart as 3.5 Å in R to 2.341 Å in TS and 1.415 Å in the products P. Simultaneously, the elongation of the C-1–O-1 bond occurs going from 1.457 Å in R to 2.662 Å in TS, and finally to 4.286 Å in P. Along the reaction pathway a conformational rearrangement of the galactopyranose ring occurs and variations in the distance C-1–O-5 and torsion angle C-5–O-5–C-1–C-2 reflect changes in the ring structure. The ring geometry in R is characterized by a C-1–O-5 bond and a C-5–O-5–C-1–C-2 angle of 1.400 Å and −58.1°, respectively. The C-1–O-5 bond in TS is shortened to 1.283 Å, and the C-5–O-5–C-1–C-2 angle changes to −22.2°, what is consistent with the charge delocalization occurring in the six-atom ring during the formation of the oxocarbenium ion. The orientation of the primary hydroxyl group characterized by a C-5–C-6 torsion angle remains in the *gg* position along the $R \rightarrow TS \rightarrow P$ pathway. It is noteworthy to comment on the role of Gln189 during the reaction. From our calculations, it appears that Gln189 is involved in the hydrogen bonding with the donor and the acceptor galactose in TS via the donor ring oxygen O-5 and the primary hydroxyl group oxygen O-6′ of the acceptor with the N_{Gln}–O-5 and N_{Gln}–O-6′ distances of about 3 Å. This implies that Gln189 participates in the stabilization of the TS. The hydrogen bonding to the O-5 is not observed in the ground state what might explain why the Q189A LgtC mutant has similar K_m value for UDP-Gal although considerably higher for lactose.[8,21] The above analysis clearly shows that the geometry of the lowest energy (most probable) transition state estimated by the B3LYP/6-31G* method is unique and is far from the transition state structures determined for inverting or retaining glycosyltransferases studied so far.[18–20]

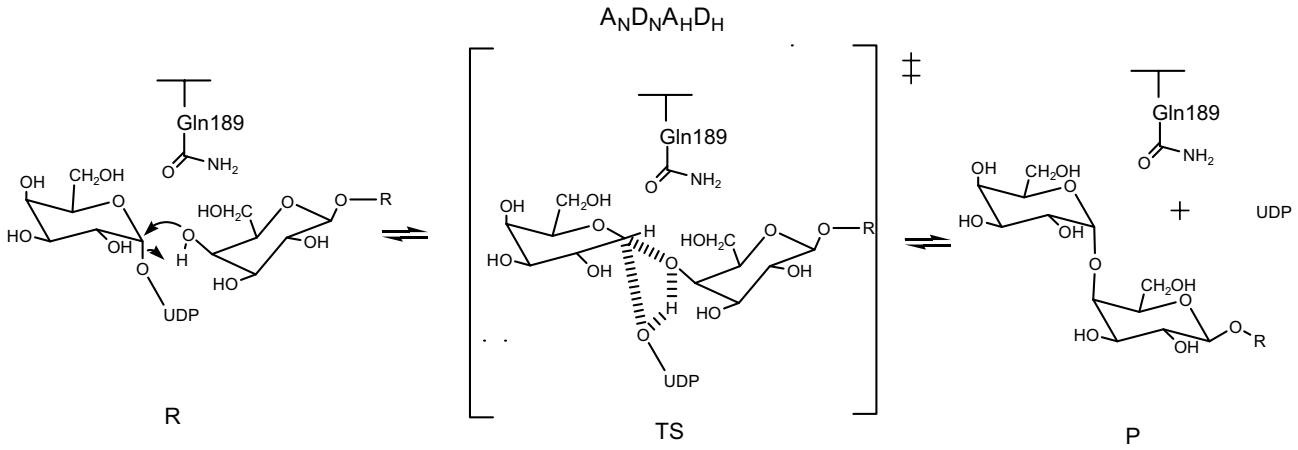

Scheme 4. Schematic representation of the predicted reaction mechanism catalyzed by LgtC.

3.3. The catalytic mechanism of LgtC inferred from molecular modeling

The B3LYP/6-31G* calculations predict that preferred reaction pathway is a one step mechanism in which the O-4′ nucleophile from the acceptor attacks the anomeric carbon of the galactopyranose residue of the donor UDP-Gal from a side of the leaving group with the simultaneous proton transfer to a phosphate oxygen. The calculated energy barrier is in reasonable agreement with that observed experimentally. This mechanism is illustrated in Scheme 4 and can be classified, in the IUPAC definition,[32,33] as being of an $A_ND_NA_HD_H$ type mechanism because the transition state has a structure in which the forming bond is shorter (~2.3 Å) compared to the distance between the leaving group and galactopyranose (~2.7 Å) and the hydroxyl proton is partially bound to the leaving group. The recently proposed mechanism that LgtC proceeds via a front side A_ND_N-like (S_Ni) attack[8] is similar to the predicted mechanism. This mechanism differs from the other mechanisms proposed for glycosyltransferases in that it does not require the presence of any catalytic amino acid in the active site. From our results, it is apparent that the active site constraints imposed by the enzyme on the substrates change the conformation of the donor UDP-Gal to the one that is suitable for the nucleophilic attack from the leaving group side. The $A_ND_NA_HD_H$ transition state is stabilized by the enzyme and by the internal low barrier hydrogen bond that precedes the proton transfer. The calculated transition state structure also emphasizes that the acceptor contributes substantially to the nature of the transition state, and the development of stable analogues of the transition state as potent inhibitors of glycosyltransferases should therefore take these characteristics into account.

In conclusion, we have presented here a theoretical study of the reaction mechanism of the bacterial glycosyltransferase LgtC, which catalyzes the transfer of a galactose residue from UDP-Gal to lactose. The results provide a valuable insight on the catalytic action of this retaining glycosyltransferase. They have clearly excluded the possibility of a double-displacement mechanism for this enzyme. The preferred pathway is predicted to proceed by an $A_ND_NA_HD_H$ type of mechanism occurring in a single step. The determined structure of the transition state is unique and provides valuable information for designing stable analogues of TS as potent inhibitors of the bacterial LgtC.

Acknowledgements

The author wish to thank Dr. Isabelle André for her valuable discussion on the mechanism of retaining glycosyltransferases, and the Scientific Grant Agency of the Ministry of Education of Slovak Republic and the Slovak Academy of Sciences, grant VEGA-2/3077/23 for support.

References

1. Vrielink, A.; Ruger, W.; Driessen, H. P. C.; Freemont, P. S. *EMBO J.* **1994**, *13*, 3413–3422.
2. Charnock, S. J.; Davies, G. J. *Biochemistry* **1999**, *38*, 6380–6385.
3. Gastinel, L. N.; Cambillau, C.; Bourne, Y. *EMBO J.* **1999**, *18*, 3546–3557.
4. Morera, S.; Imberty, A.; Aschke-Sonnenborn, U.; Ruger, W.; Freemont, P. S. *J. Mol. Biol.* **1999**, *292*, 717–730.
5. Ha, S.; Walker, D.; Shi, Y.; Walker, S. *Protein Sci.* **2000**, *9*, 1045–1052.
6. Pedersen, L. C.; Tsuchida, K.; Kitagawa, H.; Sugahara, K.; Darden, T. A.; Negishi, M. *J. Biol. Chem.* **2000**, *275*, 34580–34585.
7. Unligil, U. M.; Zhou, S.; Yuwaraj, S.; Sarkar, M.; Schachter, H.; Rini, J. M. *EMBO J.* **2000**, *19*, 5269–5280.

8. Persson, K.; Ly, H. D.; Dieckelmann, M.; Wakarchuk, W. W.; Whiters, S. G.; Strynadka, N. C. *J. Nat. Struct. Biol.* **2000**, *8*, 166–175.
9. Gastinel, L. N.; Bignon, C.; Misra, A. K.; Hindsgaul, O.; Shaper, J. H.; Joziasse, D. H. *EMBO J.* **2001**, *20*, 638–649.
10. Mulichak, A. M.; Losey, H. C.; Walsh, C. T.; Garavito, R. M. *Structure* **2001**, *9*, 547–557.
11. Patenaude, S. I.; Seto, N. O.; Borisova, S. N.; Szpacenko, A.; Marcus, S. L.; Palcic, M. M.; Evans, S. V. *Nat. Struct. Biol.* **2002**, *9*, 685–690.
12. Gibbons, B. J.; Roach, O. J.; Hurley, T. D. *J. Mol. Biol.* **2002**, *319*, 463–477.
13. Gibson, R. P.; Turkenburg, J. P.; Charnock, S. J.; Lloyd, R.; Davies, G. *J. Chem. Biol.* **2002**, *9*, 1337–1346.
14. Boix, E.; Zhang, Y.; Swaminathan, G. J.; Brew, K.; Acharya, K. R. *J. Biol. Chem.* **2002**, *277*, 28310–28318.
15. Hu, Y.; Chen, L.; Ha, S.; Gross, B.; Falcone, B.; Walker, D.; Mokhtarzadeh, M.; Walker, S. *PNAS* **2003**, *100*, 845–849.
16. Unligil, U. M.; Rini, J. M. *Curr. Opin. Struct. Biol.* **2000**, *10*, 510–517.
17. Tarbouriech, N.; Charnock, S. J.; Davies, G. J. *J. Mol. Biol.* **2001**, *314*, 655–661.
18. Tvaroška, I.; André, I.; Carver, J. P. *J. Am. Chem. Soc.* **2000**, *122*, 8762–8776.
19. Tvaroška, I.; André, I.; Carver, J. P. *Glycobiology* **2003**, *13*, 559–566.
20. André, I.; Tvaroška, I.; Carver, J. P. *Carbohydr. Res.* **2003**, *338*, 865–877.
21. Ly, H. D.; Lougheed, B.; Wakarchuk, W. W.; Withers, S. G. *Biochemistry* **2002**, *41*, 5075–5085.
22. Campbell, J. A.; Davies, G. J.; Bulone, V.; Henrissat, B. *Biochem. J.* **1997**, *326*, 929–942.
23. Sinnott, M. L. *Chem. Rev.* **1990**, *90*, 1171–1202.
24. Bock, C. W.; Katz, M. K.; Markham, G. D.; Glusker, J. P. *J Am. Chem. Soc.* **1999**, *121*, 7360–7372.
25. Jaguar 3.5, S., Inc., Portland, OR, 1998.
26. Becke, A. D. *J. Chem. Phys.* **1993**, *98*, 5648–5652.
27. Davies, G.; Sinnott, M. L.; Withers, S. G. In *Comprehensive Biological Catalysis*; Sinott, M. L., Ed.; Academic: New York, 1997; pp 119–208.
28. Cleland, W. W.; Frey, P. A.; Gerlt, J. A. *J. Biol. Chem.* **1998**, *273*, 25529–25532.
29. Bérces, A.; Whitfield, D. M.; Nukada, T. *Tetrahedron* **2001**, *57*, 477–491.
30. http://www.sao.nrc.ca/ibs/6ring/6ring.html.
31. Vocadlo, D. J.; Davie, G. J.; Laine, R.; Withers, S. G. *Nature* **2001**, *412*, 835–838.
32. Schramm, V. L.; Shi, W. *Curr. Opin. Struct. Biol.* **2001**, *11*, 657–665.
33. Guthrie, R. D.; Jencks, W. P. *Acc. Chem. Res.* **1989**, *22*, 343–349.